Investigation of Residential Building Envelope Airtightness on Operational Performance

Adam D. Wills[1], Patrique Tardif[1], Iain A. Macdonald[1], and Heather Knudsen[1]
[1]National Research Council Canada, Ottawa, Canada

Abstract

Section 9.36 of the 2015 National Building Code of Canada (NBC) provides the minimum performance requirements for new construction housing and small buildings. There are currently no prescriptive requirements for whole-building airtightness performance or testing; however, under the performance path, airtightness testing and building performance simulation can be used to obtain credits for airtight design. The purpose of this study was to examine the operational impacts of airtightness to building owners and occupants. A calibrated ESP-r model of a contemporary semi-detached building was used to explore impacts on energy consumption, utility costs and indoor environmental quality under different locations, utility rates, and air leakage scenarios. The range of airtightness considered in the study was informed by recent guarded fan depressurization test results of 34 new attached residential units from five different Ontario builders. The results demonstrate the significant impacts high air leakage can have on building operational performance.

Introduction

The Canadian Commission of Building and Fire Codes (CCBFC), which oversees the development of Canada's national model building codes, has stated in their long-term strategy (CCBFC, 2016) a plan to promote higher building efficiency through the development and implementation of tiered energy codes with the objective of achieving net-zero energy ready buildings. Two model codes currently prescribe minimum efficiency requirements for new construction in Canada: Section 9.36 of the National Building Code of Canada (NBC) (CCBFC, 2015), and the National Energy Code for Buildings (NECB) (CCBFC, 2017). Section 9.36 of the NBC provides building envelope and equipment performance minimums for housing and small buildings (three storeys or less with a footprint ≤ 600 m^2). The NECB can be applied to all new buildings, but is typically used for large commercial and institutional buildings.

The current versions of both codes provide two compliance paths: prescriptive and performance. Under the prescriptive path a builder must demonstrate that all envelope components and mechanical equipment meets or exceeds minimum performance as described in the code. The performance path is provided to allow design flexibility and greater performance trade-offs between building components. The builder must use detailed calculations, typically using building performance simulation software (BPS) benchmarked against ASHRAE Standard 140 (ASHRAE, 2011), to demonstrate their design annually consumes the same or less energy than a code-defined reference building which uses the minimum performance for all components.

Energy efficiency improvements have historically been realized in the building code through increased envelope thermal resistance minimums and improved mechanical and electrical system efficiency requirements. As these improve, the relative share of total building energy consumption attributed to infiltration will continue to increase. Section 9.36 of the 2015 NBC does not have prescriptive minimums for whole-building envelope airtightness. Under the performance path builders may conduct a blower door test per CGSB standard 149.10-M86 (CGSB, 1986) to obtain airtightness performance credits, but this is optional and instead an airtightness of 3.2 ACH @ ΔP=50 Pa may be assumed for the proposed building (or 2.5 ACH @ ΔP=50Pa if additional construction measures are incorporated in the air barrier).

Objectives

In order to consider inclusion of whole-building airtightness requirements in Section 9.36 it is imperative to estimate and analyse the potential operational and economic costs/benefits the presence of airtightness requirements may have on builders and homeowners. The objectives of this study was to use a calibrated and validated detailed BPS model of a contemporary new attached single-family home to evaluate the financial and operational impacts different envelope airtightness performance has under different location conditions and utility rates.

Methodology

Case Study Building

The semi-detached twin test house facility at the Canadian Centre for Housing Technology (CCHT), shown in *Figure 1*, was used as the test case building for this study. The facility is located in Ottawa, ON, and was constructed in

2017. It meets the criteria of the voluntary 2012 R-2000 standard (NRCan, 2012) and the Canadian Home Builders' Association's Net-Zero Labelling Program. Each unit has a liveable floor area of 75 m^2. It is therefore assumed to be representative of contemporary high-performance housing in Canada.

Figure 1 CCHT semi-detached twin test house facility.

On-site automation systems are used to schedule and control heating, cooling, and ventilation (HVAC) equipment, water draws, appliances, lighting, and interior door opening and closing. Resistor boxes provide controlled emulation of occupant sensible gains. Energy performance and interior conditions (i.e. temperature, relative humidity, electric circuit draw, etc.) of the facility are monitored using over 500 sensors installed throughout both units and across envelope assemblies. Gas, electricity, and water meters are also installed on-site and linked to the data acquisition system.

Building Performance Simulation

Simulation of the facility was carried our using a bespoke version of ESP-r V13.1.0 (Clarke, 2021) available online (GitHub, 2022). Only the west unit was modelled, and is illustrated in Figure 2. ESP-r is one of the principle simulation tools used in ASHRAE Standard 140 (ASHRAE, 2011) and therefore is compliant with 2015 NBC Section 9.36 performance path procedures.

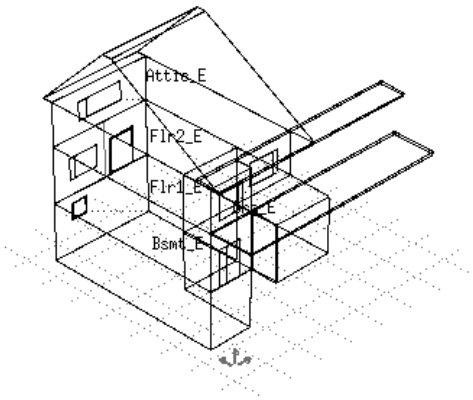

Figure 2. ESP-r model of the west unit of the CCHT facility.

The model contains five thermal zones: basement, first and second floors, attic, and garage. Two shading blocks were used to model the overhangs of the south-facing roofing, shown in Figure 2. Architectural as-built drawings were used to define the envelope materials and constructions. The effective thermal resistance of the above-grade opaque envelope are summarized in Table 1.

Table 1. Summary of effective thermal resistance of above-grade opaque envelope components

Component	RSI [m^2·K/W]	R-Value
Above-grade walls	5.20	29.5
Garage-interior partition wall	5.00	28.4
Floor header	7.08	40.2
Ceiling below attic	12.71	72.2
Exterior doors	0.93	5.3
Floor above basement	0.87	4.9

The fenestrations are triple-glazed double low-e argon filled windows with hybrid-vinyl and aluminum frames, and were modelled in the WINDOW 7.6 tool (LBNL, 2018) which yielded a centre-of-glass U-value of 0.83 W/(m^2·K) and solar heat gain coefficient (SHGC) of 0.63. The calculated fenestration performance was transferred into ESP-r.

Foundation heat loss was calculated in ESP-r using the Mitalas method (Mitalas, 1982). To define the model parameters, hourly total foundation heat loss was first calculated using the external foundation heat loss simulation tool KIVA (Kruis, 2015). Hourly above-grade foundation heat loss was then estimated using the Mitalas method assuming an above-grade three-dimensional shape factor, S_{ag}, equal to the UA-value [W/K] of the above-grade walls (ignoring corner effects). The hourly above-grade heat loss was subtracted from the total KIVA heat loss to isolate hourly below-grade heat loss. The two below-grade three-dimensional shape factors, $S_{bg,avg}$ and $S_{bg,var}$, and heat loss phase angle θ were then determined using a Fast Fourier Transform of the hourly below-grade heat loss. The Mitalas method foundation heat loss parameters for the basement of the single-unit are summarized later in Table 2. Additional details are omitted here for clarity, and the interested reader is directed to Mitalas (1982) for additional information.

Each unit is equipped with a 16.4 kW natural gas (NG) furnace with a 97% annual fuel utilization efficiency which was modelled using the empirical HVAC model developed in implemented into ESP-r by Haddad & Purdy (2003). Space cooling of the unit is provided by a whole-house air conditioner with 5.3 kW of total cooling capacity (4.0 kW sensible) and SEER and EER ratings of 16 and 13, respectively. This system was also simulated using the HVAC model from Haddad & Purdy (2003).

An energy recovery ventilator (ERV) supplied whole building ventilation to the unit. At 0 °C and -25 °C the ERV has rated sensible recovery efficiencies of 84% and 65%, respectively, with a net air flow rate of 30 L/s. Measurements from CCHT showed 34.4 L/s is achieved during operation and was used in the model. The ERV was modelled using the empirical model developed by Pinel (2014).

Facility service hot water is provided by a 50 gallon integrated heat pump hot water tank with a UEF of 3.55. This tank was modelled in ESP-r using the explicit plant network model which combines transient finite control volume and empirical solvers to model heat and mass transfer in mechanical equipment. The system was modelled using a two node stratified tank model developed by Thevenard & Haddad (2010) coupled with an empirical air-to-water heat pump model. Heat transfer to the tank is modelled as injected mass flow from the heat pump, which is a model abstraction of the wrap-around heat exchanger in the physical unit. Model parameters were defined using available measured data and parametric calibration, described in the next section. A constant COP is assumed for the model.

Finally, infiltration in the occupied zones were modelled using the empirical ESP-r implementation of the AIM-2 model from Walker & Wilson (1990). Extended from the LBNL model (Sherman & Grimsrud, 1980), this model uses typical blower door test data and an orifice leakage power law model to calculate the operational infiltration of low-rise buildings. Walker & Wilson (1990) validated their model using SF_6 tracer gas measurements conducted at the Alberta Home Heating Research facility.

Model Calibration

The service hot water system model was calibrated prior to whole-building calibration using measured data collected at test facility. Tank electrical power consumption, hot water draw, inlet and outlet temperatures, and ambient (basement) drybulb temperature data was sampled at a five-minute intervals for 24 hours. An isolated model of the tank was developed in ESP-r, and measured flow rates, inlet temperatures, and ambient temperature were defined as boundary conditions. The tank U-value [W/(m^2·K)], COP, unit electrical draw [W], and heat pump-to-water thermal transfer rate [L/s] were parametrically varied, and modelled temporal unit electrical consumption was compared to measured using the mean absolute error (MAE). Model parameters of 1.8 W/(m^2·K), 3.1, 390 W, and 0.1 L/s, respectively, yielded a model MAE of 40.5 W and 0.3% difference in total daily energy consumption.

Automated whole-building model calibration was carried out using the Non-dominated Sorting Genetic Algorithm II (NSGA-II) from Deb et al. (2002) as implemented in the Python module *pymoo* from Blank & Deb (2020). As-built architectural drawings, site evaluations, and detailed measurements provided accurate parameter inputs for several model components. Model parameters with less certainty, which are also assumed to significantly impact results, were identified as calibration parameters and are listed in Table 2.

Base values were best estimates drawn from ASHRAE Fundamentals (ASHRAE, 2009), site data, and manufacturer data. Monari &Strachan (2017) varied "fairly well know" parameters by ±15% for their calibration approach, and "more uncertain" parameters by ±80%.

Table 2. List of calibration parameters.

Parameter	Base Value	%Variation
ACH_{50}	1.55	±15%
ELA_{10}	314.7 cm	±15%
Infiltration distribution α	N/A	[0,π/2]
Infiltration distribution β	N/A	[0,π/2]
Furnace distribution α	N/A	[0,π/2]
Furnace distribution β	N/A	[0,π/2]
Furnace capacity	6.4 kW	±80%
S_{ag}	9.0 W/K	±15%
$S_{bg,avg}$	21.5 W/K	±15%
$S_{bg,var}$	12.7 W/K	±15%
θ	5.14 rad	±15%
Gypsum material density	800 kg/m^3	±15%
OSB material density	650 kg/m^3	±15%
Flooring material density	608 kg/m^3	±80%
Concrete material density	2240 kg/m^3	±80%
Floor solar absorptivity	0.85	±80%
Exterior wall solar absorptivity	0.5	±80%
Internal gain convective fraction	0.5	±80%
Ground surface albedo	0.7	±80%
Range hood flow rate	0.142 kg/s	±80%

AIM-2 requires inputs on the fractions of total leakage to the ceiling, wall, and floor (f_{ceil}, f_{wall}, and f_{floor}, respectively). These values were specified in the optimization of the independent parameters α and β which vary between 0 and π/2:

$$f_{ceil} = G \cdot \cos(\alpha) \quad (1)$$

$$f_{wall} = G \cdot \sin(\alpha) \cdot \sin(\beta) \quad (2)$$

$$f_{floor} = G \cdot \cos(\beta) \quad (3)$$

where,

$$G = \frac{1}{\cos(\alpha) + \sin(\alpha) \cdot \cos(\beta) + \cos(\beta)} \quad (4)$$

Equations similar to 1 through 4 are used to specify the distribution of heating system output to the basement, first, and second floor.

Measured five-minute data from the west unit was collected from December 21st to 31st 2019. First, second and basement floor drybulb temperatures, and hourly furnace NG consumption, were used as calibration and validation targets. Data from the 21st to the 28th was used for calibration, and data from the 29th to the 31st was used for validation.

The NSGA-II was set up to minimize the coefficient of variation of the root-mean-square error (CV(RMSE)) and normalized mean bias error (NMBE) of each calibration target, totalling in eight optimization objective functions. Hamdy et al. (2016) recommended two to four times the number of parameters for population size, and found that non-dominated solutions stabilized after 1400 to 1800 evaluations. For this optimization there are 20 parameters; thus a population of 50 was selected based on the

recommended range from Hamdy et al. (2016) and available CPUs. The number of generations was set to 32 to yield 1600 total evaluations. All other NSGA-II parameters were set to default.

The "best" point along the Pareto Front was selected using the Achievement Scalarization Function (Wierzbicki, 1980), with the NG hourly consumption CV(RMSE) and NMBE weighted four and two times the weight of the other objective functions, respectively. Calibration results are presented later in the Results section.

Economic Model

The utility rates paid by Canadian residential customers varies significantly across jurisdictions. For this analysis current and future electricity and natural gas rates reported by the Canadian Energy Regulator (CER, 2021) were used. This database provides demand-weighted $/GJ estimates for residential electricity, NG, and oil consumed for each province and territory, with annual projections out to 2050. Values are provided in real Canadian dollar with a base year of 2021; i.e. costs adjusted for inflation. Annual simulations were used to estimate annual utility costs for 2022 to 2041.

Comfort Model

The indoor thermal comfort model from Peeters et al. (2009) was used to characterize indoor conditions of the first and second floors for each location and airtightness scenario considered. Peeters et al. (2009) developed a comfort algorithms for residential buildings with a focus on interoperability with BPS tools. Different algorithms were defined for different space types (bathroom, bedroom, and other), and for a given operative temperature the algorithms provided estimates if 10% and 20% predicted percentage of dissatisfied (PPD) is true.

Given the current model is discretized by floors and not rooms/spaces, the operative temperature on each floor was assumed to be approximately equal to the drybuld temperature, and the room type of "other" was assumed. Additional comfort model details are omitted here for clarity, and the interested reader is directed to Peeters et al. (2009) for more information.

Simulation Plan and Procedures

The calibrated CCHT building model was used to simulate annual energy performance of the building under different location and envelope airtightness scenarios. Four different locations were considered:

- Vancouver, BC (Climate Zone 4);
- Toronto, ON (Climate Zone 5);
- Montréal, PQ (Climate Zone 6);
- Calgary, AB (Climate Zone 7A);

Data from the Canadian Housing and Mortgage Corporation show the provinces of British Columbia, Ontario, Québec, and Alberta accounted for 22%, 33%, 23%, and 15% of new housing completions in 2019 (CMHC, 2019), respectively. The majority of the completions in each province were in the locations selected for the study. The 2020 version of the annual hourly Canadian Weather Year for Energy Calculations data (ECCC, 2021)

For each location five envelope airtightness performance levels were evaluated: 0.6, 1.5, 2.5, 3,2, and 4.4 ACH @ ΔP=50 Pa (ACH_{50}). The 0.6 ACH_{50} performance was selected to represent Passive House requirements (PHI, 2015). The 1.5 ACH_{50} performance was selected to represent R-2000 requirements (NRCan, 2012). Both 2.5 and 3.2 ACH_{50} represent reference envelope performance in Section 9.36 in the 2015 NBC (CCBFC, 2015). The 4.4 ACH_{50} performance was derived from the largest guarded blower door test leakage measured by Rosen (2021). They conducted guarded and unguarded blower door tests of 34 row, back-to-back, and stacked townhomes built between 2019 and 2021 in Ontario. Eight units were Energy Star for New Homes, and the other 26 units were not part of any voluntary programs. The average unit guarded airtightness was 2.24 ACH_{50}, with a standard deviation of 0.68 ACH_{50}. For each airtightness scenario the default flow exponent of 0.67 was used.

The daily internal gain and hot water schedules used during testing were maintained for the simulation study. The CCHT internal gains are 9.0 kWh/day, and hot water draws are 214 L/day. Space heating and cooling was modelled as being controlled by an ON/OFF thermostat located on the first floor. The space heating setpoint was 21 °C ±0.5 °C, and space cooling was 25 °C ±0.5 °C per NBC Sentences 9.36.5.4.(5), (6), and (7). The thermostat was set to heating only for November 8th to April 1st, cooling only June 4th to September 16th. All other periods allowed both heating and cooling operation. This operation schedule is based on the Canadian residential operation schedule developed by Swan et al. (2013).

Equipment Specification & Sizing

Prior to simulating the different location and airtightness scenarios the space heating and cooling systems of the building were re-sized from the base system installed at CCHT. CWEC climate data and annual simulation were used to determine peak heating and cooling demand of the building for each location. During sizing, each of the occupied zones were controlled with an ideal zone controller which precisely maintained heating and cooling setpoints at 22 °C and 24 °C, respectively to follow CSA standard F280-2012 (CSA, 2012). The Envelope infiltration during sizing was set to 3.57 ACH_{50} which is the default value for current construction in the standard. Internal gains, service hot water operation, and ventilation were not altered for sizing.

Results

Whole-Building Calibration

Table 3 provides the CV(RMSE) and NMBE values of the calibrated model for the calibration simulation period. Also provided are the MAE values. The hourly furnace NG

consumption CV(RMSE) and NMBE are shown to be within the limits of hourly calibrated model estimates as specified by ASHRAE Guideline 14 (ASHRAE, 2014), which are 30% and 10%, respectively.

Table 3. Calibration period model performance

Target	CV(RMSE)	NMBE	MAE
Main floor temperature	3.0%	-2.3%	0.6 °C
Second floor temperature	8.0%	6.7%	1.5 °C
Basement temperature	4.9%	2.0%	0.8 °C
Hourly furnace NG consumption	27.7%	3.5%	0.04 m^3 [1.3 ft^3]

Table 4 provides the calibrated model error values for the validation period.

Table 4. Validation period model performance

Target	CV(RMSE)	NMBE	MAE
Main floor temperature	2.8%	-2.2%	0.5 °C
Second floor temperature	8.2%	7.1%	1.5 °C
Basement temperature	4.9%	3.3%	0.8 °C
Hourly furnace NG consumption	28.5%	-4.1%	0.04 m^3 [1.3 ft^3]

It can be seen that the hourly furnace NG consumption CV(RMSE) and NMBE values still comply with ASHRAE Guideline 14.

Sizing

Table 5 provides the peak sensible space heating and cooling demands determined during the sizing simulations.

Table 5. Peak heating and cooling demand.

Location	Peak Sensible Heating [kW]	Peak Sensible Cooling [kW]
Vancouver	6.0	1.7
Toronto	8.3	2.0
Montréal	8.7	2.4
Calgary	8.1	2.5

For each location the space heating system was modelled with a capacity equal to those listed in Table 5. Vancouver, Toronto, and Calgary were modelled with NG furnaces with an annual fuel utilization efficiency of 97%, and for Montréal an electric furnace was modelled. The central air source heat pump cooling system installed at CCHT, described previously, was modelled for all location scenarios since the capacity is sufficient.

Energy & Utility Costs Analysis

Figures 3 & 4 plot the annual building site end-use energy consumption for space heating and cooling, respectively. NG consumption was expressed in MWh by assuming the ESP-r default heating value of 10.3 kWh/m^3. Figure 3 shows that for all locations increasing envelope airtightness reduces annual space heating energy consumption. Figure 4 shows that space cooling energy consumption increases with envelope airtightness with the exception of Montréal which does not vary notably with airtightness.

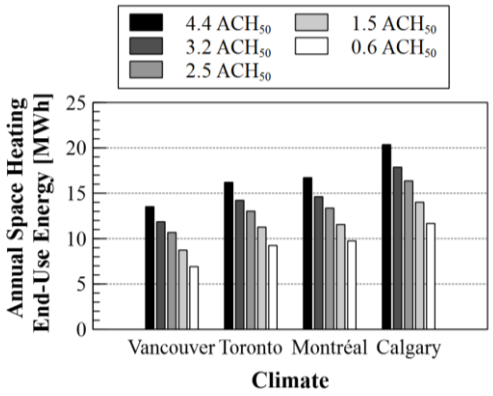

Figure 3. Annual site energy consumption for space heating.

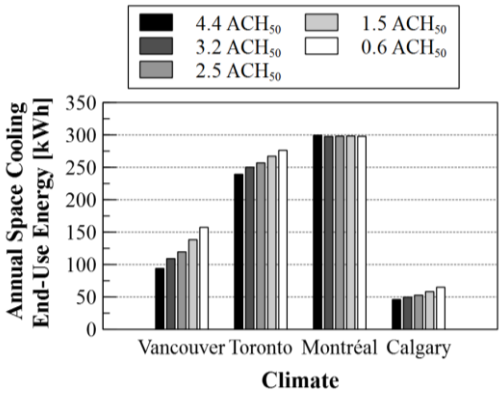

Figure 4. Annual site energy consumption for space cooling.

Figures 5 to 8 plot the cumulative annual utility cost projections for space heating and cooling end-uses for Vancouver, Toronto, Montréal, and Calgary, respectively. Estimates span 20 years from 2022 to 2041, and are expressed in units of $1k 2021 Canadian dollars.

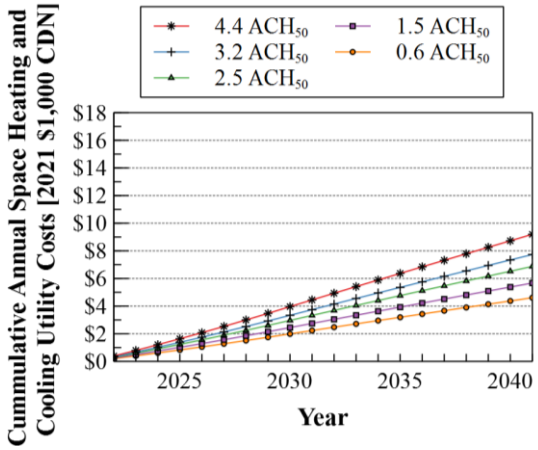

Figure 5. Estimated cumulative annual space heating and cooling utility cost projections for Vancouver.

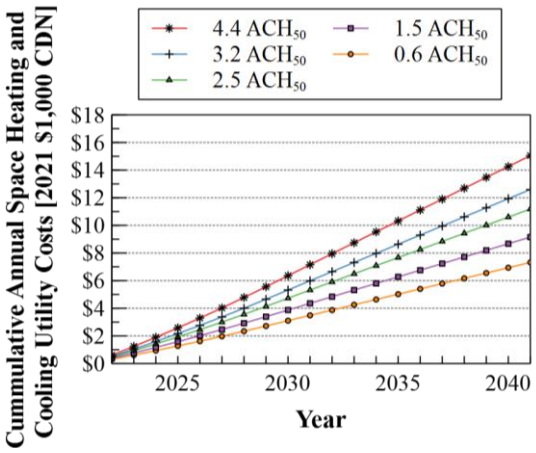

Figure 6. Estimated cumulative annual space heating and cooling utility cost projections for Toronto.

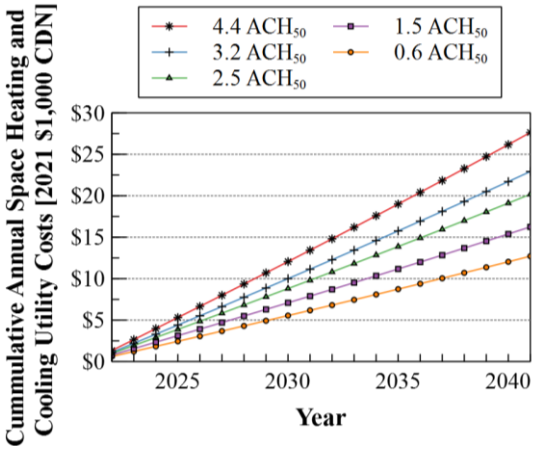

Figure 7. Estimated cumulative annual space heating and cooling utility cost projections for Montréal.

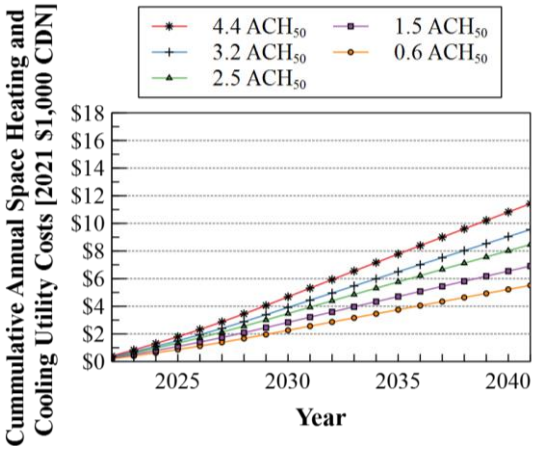

Figure 8. Estimated cumulative annual space heating and cooling utility cost projections for Calgary.

It can be seen that for all locations the cumulative annual space heating and cooling utility cost projections reduce with increasing airtightness performance. The energy cost projections used from CER (2021) assumes that in 2030 the current carbon pricing policy affecting NG ends and is not replaced.

Comfort Analysis

Thermal comfort of the second floor was analysed since heating and cooling of the space was indirectly controlled by the first floor thermostat. It was found that for all locations and airtightness scenarios the cumulative hours of 20% PPD for it being too warm was approximately zero for the first floor. The only exception was Toronto, which had 20 cumulative minutes where 20% PPD for it being too warm for the 3.2 ACH_{50} scenario, up to 6 cumulative hours for 0.6 ACH_{50}.

Figures 9 & 10 plot the total hours of the year 20% of people would be predicted to be too warm and too cold on the second floor, respectively.

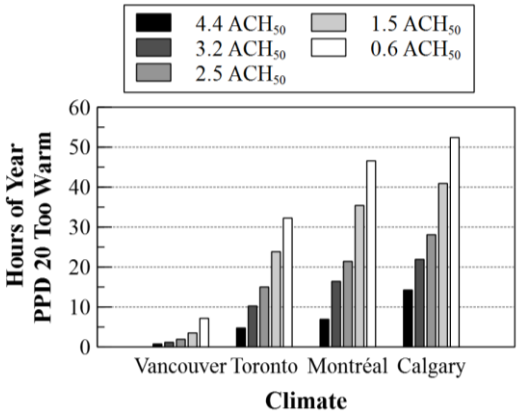

Figure 9. Hours of year 20% PPD too warm on second floor.

Figure 9 shows that the cumulative time the second floor is too warm increases with both ACH_{50} as well as heating degree days. Figure 10 shows that the cumulative annual time the second floor is too cold decreases with ACH_{50} for all locations. Comparing the y-axes of Figures 9 & 10 it can be seen that the cumulative time the second floor is too cold is an order of magnitude larger than cumulative time the space is too warm.

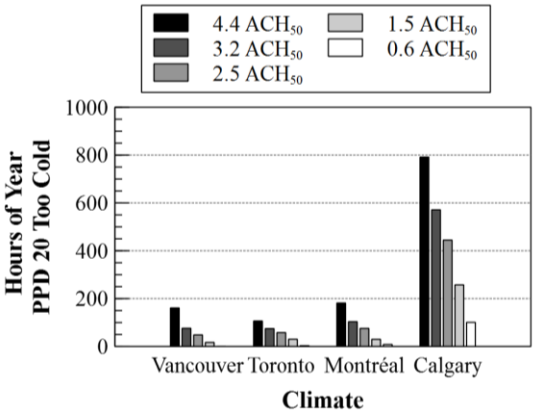

Figure 10. Fraction of year 20% PPD too cold on second floor.

Discussion

Figure 3 shows that increasing envelope airtightness reduces the amount of annual energy consumption for space heating for all locations considered. This was expected since higher envelope airtightness reduces infiltration of cold outdoor air during the heating season. Figure 4, however, shows that reducing infiltration increases the cooling load since during the cooling season the building is less able to benefit from "free cooling" of outdoor air during times of high internal and solar gains. Therefore, by increasing envelope airtightness there is a trade-off between heating and cooling energy consumption savings.

Canadian residential buildings are still heating dominated, as illustrated by comparison of the relatively large annual space heating energy consumptions in Figure 3 and the space cooling consumptions in Figure 4. Figures 5 to 8 illustrate that for each location considered that there is a net-benefit in terms of annual utility costs for increased envelope airtightness. Figures 5 to 8 also illustrate how the cumulative savings in utility costs increases over time for each location and airtightness performance.

Since energy costs projections out to 2041 have a relatively high level of uncertainty, Table 6 summarizes the cumulative utility savings from 2022 to 2031 (10 years), relative to the 2.5 ACH_{50} scenario (the implicit code reference airtightness performance).

Table 6. Cumulative utility savings over 10 years, relative to 2.5 ACH_{50}

Location	4.4 ACH_{50}	3.2 ACH_{50}	1.5 ACH_{50}	0.6 ACH_{50}
Vancouver	-$1,121	-$415	$582	$1,094
Toronto	-$1,834	-$669	$963	$1,833
Montréal	-$3,621	-$1,333	$1,911	$3,629
Calgary	-$1,374	-$503	$722	$1,371

Montréal is shown to have the largest variation in cumulative utility cost savings across the airtightness scenarios compared to other locations. This is due to the other locations using relatively less expensive NG for space heating demands, whereas the Montréal scenario assumes an electric furnace.

Figures 5 to 8 and Table 6 demonstrate that, for example, an undetected defect in a building envelope causing increased infiltration will have operational cost implications for homeowners. Without a blower door test it is unlikely a homeowner would be aware their envelope is performing below code-reference, and therefore unlikely to address envelope defects and incur higher utility costs.

In order to establish the potential savings of improving airtightness for a specific home, the baseline performance must first be measured. The baseline then informs the potential savings, and considered alongside the associated labour and material capital costs to implement the specific envelop alterations required, cost benefit and simple payback may be determined.

One concern of higher envelope airtightness is the risk of overheating. Thermal conditions of the second floor were analysed since the first floor contains the thermostat, and thermal conditions on that floor were therefore assumed to be maintained by the heating and cooling equipment. Figure 9 showed that the second floor experienced more periods of higher than comfortable temperatures (PPD 20%) as airtightness increased. Figure 10, however, showed that the cumulative time the second floor was too cold (PPD 20%) decreases with increasing airtightness.

Comparing Figure 10 to Figure 9 it can be seen that for each location the cumulative times the second floor is too cold are orders of magnitude larger than the cumulative time they are too warm. These results suggest there is a net-benefit in thermal comfort improvement by increasing envelope airtightness performance, since the reduction in cumulative time the space is too cold is much greater than increase in cumulative time the space is too warm for each location.

Conclusions

The calibrated model of the high-performance CCHT semi-detached twin test facility was used as a sandbox for exploring the operational costs and comfort impacts of envelope airtightness performance for different locations. The results of the analysis demonstrate that while increasing airtightness increases the cooling load in all locations, it is offset by the annual space heating energy savings, and net-savings for utility costs in all locations. Similarly, the analysis demonstrated that increased airtightness increases the cumulative time internal temperatures are perceived as too warm, it is offset by relatively large reductions in cumulative time the interior is perceived as too cold

Future Work

Future work will consider the impacts of climate change on projected performance and utility costs. When data becomes available, calibration and validation of the CCHT under cooling operation will be also conducted. Finally, future work will examine the impact of indoor air contaminant concentrations under different envelope airtightness performance scenarios.

References

ASHRAE. (2009). ASHRAE Handbook: Fundamentals. Atlanta: American Society of Heating, Refrigerating and Air-Conditioning Engineers, Inc.

ASHRAE. (2011). ANSI/ASHRAE 140 Standard Method of Test for the Evaluation of Building Energy Analysis Computer Programs. Atlanta: American Society of Heating, Refrigerating and Air-Conditioning Engineers.

ASHRAE. (2014). ASHRAE Guideline 14: Measurement of Energy, Demand, and Water Savings. Atlanta: American Society of Heating, Refrigerating and Air-Conditioning Engineers.

Blank, J., & Deb, K. (2020). pymoo: Multi-Objective Optimization in Python. IEEE Access, 8, 89497-89509.

CCBFC. (2015). National Building Code of Canada. Ottawa: National Research Council of Canada.

CCBFC. (2016). Long-Term Strategy for Developing and Implementing More Ambitious Energy Codes: A Position Paper. Ottawa, ON: Canadian Commission on Building and Fire Codes.

CCBFC. (2017). National Energy Code of Canada for Buildings. Ottawa: National Research Council Canada, Codes Canada.

CER. (2021). End-Use Prices. (Canada Energy Regulator) Retrieved February 3, 2022, from Canada's Energy Future 2021: Energy Supply and Demand Projections to 2050: https://apps.cer-rec.gc.ca/ftrppndc/dflt.aspx?GoCTemplateCulture=en-CA

CGSB. (1986). CAN/CGSB-149.10-M86 Determination of the airtightness of building envelopes by the fan depressurization method. Ottawa: Canadian General Standards Board.

Clarke, J. A. (2021). ESP-r. (Energy Systems Reseach Unit, University of Strathclyde) Retrieved January 27, 2022, from https://www.strath.ac.uk/research/energysystemsresearchunit/applications/esp-r/

CMHC. (2019). Housing Market Indicators. Retrieved March 6, 2019, from Canada Mortgage and Housing Corporation: https://www.cmhc-schl.gc.ca/en/data-and-research/data-tables/housing-market-indicators

CSA. (2012). F280: Determining the required capacity of residential space heating and cooling appliances. Mississauga: Canadian Standards Association.

Deb, K., Pratap, A., Agarwal, S., & Meyarivan, T. (2002). A fast and elitist multiobjective genetic algorithm: NSGA-II. IEEE Transactions on Evolutionary Computation, 6(2), 182-197.

ECCC. (2021). Engineering Climate Datasets. (Government of Canada) Retrieved May 31, 2018, from Environment and Climate Change Canada: https://climate.weather.gc.ca/prods_servs/engineering_e.html

GitHub. (2022). Commit 71a04d3. Retrieved from ESP-r: An integrated building performance simulation program: https://github.com/AdamWillz/ESP-rSource/tree/int_hp_dhw

Haddad, K., & Purdy, J. (2003). Modeling HVAC Systems in HOT3000. Ottawa: NRCan CanmetENERGY.

Hamdy, M., Nguyen, A.-T., & Hensen, J. L. (2016). A performance comparison of multi-objective optimization algorithms for solving nearly-zero-energy-building design problems. Energy and Buildings, 121, 57-71.

Kruis, N. (2015). Development and Application of a Numerical Framework for Improving Building Foundation Heat Transfer Calculations. Boulder: Department of Civil, Environmental, and Architectural Engineering.

LBNL. (2018). WINDOW: A computer program for calculating total window thermal performance indices. (Lawrence Berkeley National Laboratory) Retrieved Mar 19, 2018, from Windows & Daylighting, Building Technology & Urban Systems Division, Energy Technologies Area: https://windows.lbl.gov/software/window

Mitalas, G. P. (1982). Calculation of below-grade residential heat loss at DBR-NRC. Ottawa: National Research Council Canada.

Monari, F., & Strachan, P. (2017). CALIBRO: an R package for the automatic calibration of building energy simulation models. Proceedings of the 15th IBPSA Conference (pp. 848-857). San Francisco: International Building Performance Simulation Association.

NRCan. (2012). R-2000 Standard. Ottawa: Natural Resources Canada.

Peeters, L., De Dear, R., Hensen, J., & D'haeseleer, W. (2009). Thermal comfort in residential buildings: Comfort values and scales for building energy simulation. Applied Energy, 86(5), 772-780.

PHI. (2015). Passive House requirements. Retrieved from www.passiv.de/en/

Pinel, P. (2014). Development of an ERV model for ESP-r. Ottawa: Natural Resources Canada.

Rosen, M. (2021). Airtightness of attached homes: Phase 3 data collection & analysis. Ottawa: Building Energy Inc.

Sherman, M. H., & Grimsrud, D. T. (1980). Infiltration-Pressurization Correlation: Simplified Physical Modelling. Berkeley, CA: Lawrence Berkeley Laboratory, University of California.

Swan, L. G., Ugursal, V. I., & Beausoleil-Morrison, I. (2013). Hybrid residential end-use energy and greenhouse gas emissions model–development and verification for Canada. Journal of Building Performance Simulation, 1-23.

Thevenard, D., & Haddad, K. (2010). Development of a stratified tank model with immersed heat exchangers in ESP-r. Proceedings of eSim 2010 (pp. 9-16). Winnipeg: International Building Performance Simulation Association.

Walker, I., & Wilson, D. (1990). The Alberta Air Infiltration Model: AIM-2. Edmonton: University of Alberta, Department of Mechanical Engineering.

Wierzbicki, A. P. (1980). The use of reference objectives in multiobjective optimization. Multiple criteria decision making theory and application, 468-486.